Search for Dark Matter Annihilations towards the Inner Galactic Halo from 10 Years of Observations with H.E.S.S.

H. Abdallah,[1] A. Abramowski,[2] F. Aharonian,[3,4,5] F. Ait Benkhali,[3] A. G. Akhperjanian,[5,6] E. Angüner,[7] M. Arrieta,[8] P. Aubert,[9] M. Backes,[10] A. Balzer,[11] M. Barnard,[1] Y. Becherini,[12] J. Becker Tjus,[13] D. Berge,[14] S. Bernhard,[15] K. Bernlöhr,[3,7] E. Birsin,[7] R. Blackwell,[16] M. Böttcher,[1] C. Boisson,[8] J. Bolmont,[17] P. Bordas,[18] J. Bregeon,[19] F. Brun,[20] P. Brun,[20] M. Bryan,[11] T. Bulik,[21] M. Capasso,[22] J. Carr,[23] S. Casanova,[24,3] N. Chakraborty,[3] R. Chalme-Calvet,[17] R. C. G. Chaves,[19] A. Chen,[25] J. Chevalier,[9] M. Chrétien,[17] S. Colafrancesco,[25] G. Cologna,[26] B. Condon,[27] J. Conrad,[28,29] C. Couturier,[17] Y. Cui,[18] I. D. Davids,[10,1] B. Degrange,[22] C. Deil,[3] P. deWilt,[16] A. Djannati-Ataï,[30] W. Domainko,[3] A. Donath,[3] L. O'C. Drury,[4] G. Dubus,[31] K. Dutson,[32] J. Dyks,[33] M. Dyrda,[24] T. Edwards,[3] K. Egberts,[34] P. Eger,[3] J.-P. Ernenwein,[35] S. Eschbach,[35] C. Farnier,[28] S. Fegan,[22] M. V. Fernandes,[2] A. Fiasson,[9] G. Fontaine,[22] A. Förster,[3] S. Funk,[36] M. Füßling,[34] S. Gabici,[30] M. Gajdus,[7] Y. A. Gallant,[19] T. Garrigoux,[1] G. Giavitto,[37] B. Giebels,[22] J. F. Glicenstein,[20] D. Gottschall,[18] A. Goyal,[38] M.-H. Grondin,[27] M. Grudzińska,[21] D. Hadasch,[15] J. Hahn,[3] J. Hawkes,[16] G. Heinzelmann,[2] G. Henri,[31] G. Hermann,[3] O. Hervet,[8] A. Hillert,[3] J. A. Hinton,[3,32] W. Hofmann,[3] C. Hoischen,[37] M. Holler,[22] D. Horns,[2] A. Ivascenko,[1] A. Jacholkowska,[17] M. Jamrozy,[38] M. Janiak,[33] D. Jankowsky,[39] F. Jankowsky,[26] M. Jingo,[25] T. Jogler,[39] L. Jouvin,[40] I. Jung-Richardt,[36] M. A. Kastendieck,[2] K. Katarzyński,[41] U. Katz,[36] D. Kerszberg,[17] B. Khélifi,[30] M. Kieffer,[17] J. King,[3] S. Klepser,[37] D. Klochkov,[18] W. Kluźniak,[33] D. Kolitzus,[42] Nu. Komin,[25] K. Kosack,[20] S. Krakau,[13] M. Kraus,[39] F. Krayzel,[9] P. P. Krüger,[1] H. Laffon,[27] G. Lamanna,[9] J. Lau,[16] J.-P. Lees,[43] J. Lefaucheur,[8] V. Lefranc,[20,†,‡] A. Lemière,[30] M. Lemoine-Goumard,[27] J.-P. Lenain,[17] E. Leser,[34] T. Lohse,[7] M. Lorentz,[20] R. Lui,[3] I. Lypova,[37] V. Marandon,[3] A. Marcowith,[19] C. Mariaud,[22] R. Marx,[3] G. Maurin,[9] N. Maxted,[16] M. Mayer,[34] P. J. Meintjes,[44] U. Menzler,[13] M. Meyer,[28] A. M. W. Mitchell,[3] R. Moderski,[33] M. Mohamed,[26] K. Morå,[28] E. Moulin,[20,†,§] T. Murach,[7] M. de Naurois,[22] F. Niederwanger,[14] J. Niemiec,[24] L. Oakes,[7] H. Odaka,[3] S. Ohm,[37] S. Öttl,[42] M. Ostrowski,[38] I. Oya,[7] M. Padovani,[45] M. Panter,[3] R. D. Parsons,[3] M. Paz Arribas,[7] N. W. Pekeur,[1] G. Pelletier,[31] P.-O. Petrucci,[31] B. Peyaud,[20] S. Pita,[30] H. Poon,[3] D. Prokhorov,[12] H. Prokoph,[12] G. Pühlhofer,[18] M. Punch,[30] A. Quirrenbach,[26] S. Raab,[36] A. Reimer,[42] O. Reimer,[42] M. Renaud,[19] R. de los Reyes,[3] F. Rieger,[3] C. Romoli,[4] S. Rosier-Lees,[9] G. Rowell,[16] B. Rudak,[33] C. B. Rulten,[8] V. Sahakian,[5,6] D. Salek,[46] D. A. Sanchez,[9] A. Santangelo,[18] M. Sasaki,[18] R. Schlickeiser,[13] F. Schüssler,[20] A. Schulz,[37] U. Schwanke,[7] S. Schwemmer,[26] A. S. Seyffert,[1] N. Shafi,[25] R. Simoni,[14] H. Sol,[8] F. Spanier,[1] G. Spengler,[28] F. Spieß,[2] L. Stawarz,[38] R. Steenkamp,[10] C. Stegmann,[34,37] F. Stinzing,[36,*] K. Stycz,[37] I. Sushch,[47] J.-P. Tavernet,[17] T. Tavernier,[30] A. M. Taylor,[4] R. Terrier,[30] M. Tluczykont,[2] C. Trichard,[9] R. Tuffs,[3] J. van der Walt,[1] C. van Eldik,[36] B. van Soelen,[44] G. Vasileiadis,[19] J. Veh,[36] C. Venter,[47] A. Viana,[3] P. Vincent,[17] J. Vink,[11] F. Voisin,[16] H. J. Völk,[3] T. Vuillaume,[9] Z. Wadiasingh,[47] S. J. Wagner,[26] P. Wagner,[7] R. M. Wagner,[28] R. White,[32,3] A. Wierzcholska,[38] P. Willmann,[36] A. Wörnlein,[36] D. Wouters,[20] R. Yang,[3] V. Zabalza,[3,32] D. Zaborov,[22] M. Zacharias,[26] A. A. Zdziarski,[33] A. Zech,[8] F. Zefi,[22] A. Ziegler,[36] and N. Żywucka[38]

(H.E.S.S. Collaboration)

[1]*Centre for Space Research, North-West University, Potchefstroom 2520, South Africa*
[2]*Universität Hamburg, Institut für Experimentalphysik, Luruper Chaussee 149, D 22761 Hamburg, Germany*
[3]*Max-Planck-Institut für Kernphysik, P.O. Box 103980, D 69029 Heidelberg, Germany*
[4]*Dublin Institute for Advanced Studies, 31 Fitzwilliam Place, Dublin 2, Ireland*
[5]*National Academy of Sciences of the Republic of Armenia, Marshall Baghramian Avenue, 24, 0019 Yerevan, Republic of Armenia*
[6]*Yerevan Physics Institute, 2 Alikhanian Brothers Street, 375036 Yerevan, Armenia*
[7]*Institut für Physik, Humboldt-Universität zu Berlin, Newtonstrasse 15, D 12489 Berlin, Germany*
[8]*LUTH, Observatoire de Paris, PSL Research University, CNRS, Université Paris Diderot, 5 Place Jules Janssen, 92190 Meudon, France*
[9]*Laboratoire d'Annecy-le-Vieux de Physique des Particules, Université de Savoie, CNRS/IN2P3, F-74941 Annecy-le-Vieux, France*
[10]*University of Namibia, Department of Physics, Private Bag 13301, Windhoek, Namibia*
[11]*GRAPPA, Anton Pannekoek Institute for Astronomy, University of Amsterdam, Science Park 904, 1098 XH Amsterdam, The Netherlands*
[12]*Department of Physics and Electrical Engineering, Linnaeus University, 351 95 Växjö, Sweden*
[13]*Institut für Theoretische Physik, Lehrstuhl IV: Weltraum und Astrophysik, Ruhr-Universität Bochum, D 44780 Bochum, Germany*

[14]GRAPPA, Anton Pannekoek Institute for Astronomy and Institute of High-Energy Physics, University of Amsterdam, Science Park 904, 1098 XH Amsterdam, The Netherlands
[15]Institut für Astro- und Teilchenphysik, Leopold-Franzens-Universität Innsbruck, A-6020 Innsbruck, Austria
[16]School of Chemistry & Physics, University of Adelaide, Adelaide 5005, Australia
[17]LPNHE, Université Pierre et Marie Curie Paris 6, Université Denis Diderot Paris 7, CNRS/IN2P3, 4 Place Jussieu, F-75252, Paris Cedex 5, France
[18]Institut für Astronomie und Astrophysik, Universität Tübingen, Sand 1, D 72076 Tübingen, Germany
[19]Laboratoire Univers et Particules de Montpellier, Université Montpellier 2, CNRS/IN2P3, CC 72, Place Eugène Bataillon, F-34095 Montpellier Cedex 5, France
[20]DSM/Irfu, CEA Saclay, F-91191 Gif-Sur-Yvette Cedex, France
[21]Astronomical Observatory, The University of Warsaw, Aleje Ujazdowskie 4, 00-478 Warsaw, Poland
[22]Laboratoire Leprince-Ringuet, Ecole Polytechnique, CNRS/IN2P3, F-91128 Palaiseau, France
[23]Aix Marseille Université, CNRS/IN2P3, CPPM UMR 7346, 13288 Marseille, France
[24]Instytut Fizyki Jądrowej PAN, ul. Radzikowskiego 152, 31-342 Kraków, Poland
[25]School of Physics, University of the Witwatersrand, 1 Jan Smuts Avenue, Braamfontein, Johannesburg 2050, South Africa
[26]Landessternwarte, Universität Heidelberg, Königstuhl, D 69117 Heidelberg, Germany
[27]Université Bordeaux 1, CNRS/IN2P3, Centre d'Études Nucléaires de Bordeaux Gradignan, 33175 Gradignan, France
[28]Oskar Klein Centre, Department of Physics, Stockholm University, Albanova University Center, SE-10691 Stockholm, Sweden
[29]Wallenberg Academy Fellow
[30]APC, AstroParticule et Cosmologie, Université Paris Diderot, CNRS/IN2P3, CEA/Irfu, Observatoire de Paris, Sorbonne Paris Cité, 10, rue Alice Domon et Léonie Duquet, 75205 Paris Cedex 13, France
[31]UJF-Grenoble 1 / CNRS-INSU, Institut de Planétologie et d'Astrophysique de Grenoble (IPAG) UMR 5274, Grenoble F-38041, France
[32]Department of Physics and Astronomy, The University of Leicester, University Road, Leicester LE1 7RH, United Kingdom
[33]Nicolaus Copernicus Astronomical Center, ul. Bartycka 18, 00-716 Warsaw, Poland
[34]Institut für Physik und Astronomie, Universität Potsdam, Karl-Liebknecht-Strasse 24/25, D 14476 Potsdam, Germany
[35]Aix Marseille Universié, CNRS/IN2P3, CPPM UMR 7346, 13288 Marseille, France
[36]Universität Erlangen-Nürnberg, Physikalisches Institut, Erwin-Rommel-Strasse 1, D 91058 Erlangen, Germany
[37]DESY, D-15738 Zeuthen, Germany
[38]Obserwatorium Astronomiczne, Uniwersytet Jagielloński, ulica Orla 171, 30-244 Kraków, Poland
[39]Universität Erlangen-Nürnberg, Physikalisches Institut, Erwin-Rommel-Strasse 1, D 91058 Erlangen, Germany
[40]APC, AstroParticule et Cosmologie, Université Paris Diderot, CNRS/IN2P3, CEA/Irfu, Observatoire de Paris, Sorbonne Paris Cité, 10, rue Alice Domon et Léonie Duquet, 75205 Paris Cedex 13, France
[41]Centre for Astronomy, Nicolaus Copernicus University, ulica Gagarina 11, 87-100 Toruń, Poland
[42]Institut für Astro- und Teilchenphysik, Leopold-Franzens-Universität Innsbruck, A-6020 Innsbruck, Austria
[43]Laboratoire d'Annecy-le-Vieux de Physique des Particules, Université Savoie Mont-Blanc, CNRS/IN2P3, F-74941 Annecy-le-Vieux, France
[44]Department of Physics, University of the Free State, P.O. Box 339, Bloemfontein 9300, South Africa
[45]Laboratoire Univers et Particules de Montpellier, Université Montpellier, CNRS/IN2P3, CC 72, Place Eugène Bataillon, F-34095 Montpellier Cedex 5, France
[46]GRAPPA, Institute of High-Energy Physics, University of Amsterdam, Science Park 904, 1098 XH Amsterdam, The Netherlands
[47]Centre for Space Physics, North-West University, Potchefstroom 2520, South Africa

(Received 21 March 2016; revised manuscript received 24 May 2016; published 8 September 2016)

The inner region of the Milky Way halo harbors a large amount of dark matter (DM). Given its proximity, it is one of the most promising targets to look for DM. We report on a search for the annihilations of DM particles using γ-ray observations towards the inner 300 pc of the Milky Way, with the H.E.S.S. array of ground-based Cherenkov telescopes. The analysis is based on a 2D maximum likelihood method using Galactic Center (GC) data accumulated by H.E.S.S. over the last 10 years (2004–2014), and does not show any significant γ-ray signal above background. Assuming Einasto and Navarro-Frenk-White DM density profiles at the GC, we derive upper limits on the annihilation cross section $\langle\sigma v\rangle$. These constraints are the strongest obtained so far in the TeV DM mass range and improve upon previous limits by a factor 5. For the Einasto profile, the constraints reach $\langle\sigma v\rangle$ values of 6×10^{-26} cm^3 s^{-1} in the W^+W^- channel for a DM particle mass of 1.5 TeV, and 2×10^{-26} cm^3 s^{-1} in the $\tau^+\tau^-$ channel for a 1 TeV mass. For the first time, ground-based γ-ray observations have reached sufficient sensitivity to probe $\langle\sigma v\rangle$ values expected from the thermal relic density for TeV DM particles.

DOI: 10.1103/PhysRevLett.117.111301

Introduction.—About 85% of the mass content of the Universe is composed of cold nonbaryonic dark matter (DM) [1]. There are many well-motivated elementary particle candidates arising in extensions of the standard model of particle physics. One of the most compelling classes of models assumes DM to consist of weakly interacting massive particles (WIMPs) [2–4]: stable particles with masses and coupling strengths at the electroweak scale, and produced in a standard thermal history of the Universe, have the relic density that corresponds to that of observed DM. WIMPs would today self-annihilate in high DM density regions producing standard model particles, including a potential continuum emission of very-high-energy (VHE, $E_\gamma \gtrsim 100$ GeV) γ rays in the final state that can be detected by the H.E.S.S. (High Energy Stereoscopic System) array of ground-based Cherenkov telescopes.

Observational strategies to search for DM annihilation signals focus on regions in the sky with both expected high DM density and reduced astrophysical γ-ray signals. VHE γ-ray observations of the Galactic Center (GC) region are amongst the most promising avenues to look for DM annihilation signals due to the GC proximity and its expected large DM content. DM annihilation signals from the GC are expected to be stronger than those from dwarf galaxies by several orders of magnitudes. However, contrary to the case of dwarf galaxies, observations of the GC region face strong astrophysical backgrounds. Indeed, the inner 300 pc of the GC harbors VHE emitters, namely, the central γ-ray source HESS J1745-290 [5,6], the supernova or pulsar wind nebula G0.9 + 0.1 [7], the supernova remnant HESS J1745-303 [8], and a diffuse emission extending along the Galactic plane [9]. For DM particles in the TeV mass range, the strongest constraints on the velocity-weighted annihilation cross section $\langle\sigma v\rangle$ to date lie at 3×10^{-25} cm^3 s^{-1} from 112 h of observation towards the GC region by H.E.S.S. and a parametrization of the γ-ray annihilation spectrum via $q\bar{q}$ pairs [10].

The differential γ-ray flux from the self-annihilation of DM particles of mass $m_{\rm DM}$ in a solid angle $\Delta\Omega$ is given by

$$\frac{d\Phi_\gamma}{dE_\gamma}(E_\gamma, \Delta\Omega) = \frac{\langle\sigma v\rangle}{8\pi m_{\rm DM}^2}\frac{dN_\gamma}{dE_\gamma}(E_\gamma) \times J(\Delta\Omega)$$
$$\text{with} \quad J(\Delta\Omega) = \int_{\Delta\Omega}\int_{\rm LOS} ds\, d\Omega \rho^2(r(s,\theta)). \qquad (1)$$

The particle physics properties are encapsulated in the first term where $\langle\sigma v\rangle$ is the thermally averaged velocity-weighted annihilation cross section, and $dN_\gamma/dE_\gamma(E_\gamma) = \sum_f B_f dN_\gamma^f/dE_\gamma(E_\gamma)$ is the total differential γ-ray yield per annihilation, which corresponds to the sum of the differential γ-ray yields over the final states f with branching ratio B_f. (Only prompt emission of γ rays is considered here. Secondary emission is expected from the inverse Compton scattering of energetic electrons produced in the DM annihilation on ambient radiation fields. This is particularly relevant in the lepton channels as shown in Ref. [11].) The function $J(\Delta\Omega)$, referred to hereafter as the J factor, integrates the square of the DM density ρ along the line of sight (LOS) in a solid angle $\Delta\Omega$. The coordinate r reads $r = (r_\odot^2 + s^2 - 2r_\odot s\cos\theta)^{1/2}$, where s is the distance along the line of sight, θ is the angle between the direction of observation and the Galactic Center, and $r_\odot$ is the distance of the observer to the GC assumed to be 8.5 kpc. In this analysis, the DM density distribution is parametrized with cuspy profiles. Cored profiles are not considered here. They require specific data taking and analysis methods as shown in Ref. [12]. Cuspy profiles are commonly described by Einasto [13] or Navarro-Frenk-White (NFW) [14] parametrizations, given by

$$\rho_E(r) = \rho_s \exp\left\{-\frac{2}{\alpha_s}\left[\left(\frac{r}{r_s}\right)^{\alpha_s} - 1\right]\right\}$$
$$\text{and} \quad \rho_{\rm NFW}(r) = \rho_s\left[\frac{r}{r_s}\left(1 + \frac{r}{r_s}\right)^2\right]^{-1}, \qquad (2)$$

respectively. The Einasto and NFW profile parameters (ρ_s, α_s, r_s) and (ρ_s, r_s) are extracted from Ref. [10] assuming a local DM density of $\rho_\odot = 0.39$ GeV cm^{-3}. The J factors computed in a circular region of 1° radius excluding a ±0.3° band in Galactic latitudes to avoid the above-mentioned standard astrophysical emissions give $J_E = 4.92 \times 10^{21}$ GeV^2 cm^{-5} and $J_{\rm NFW} = 2.67 \times 10^{21}$ GeV^2 cm^{-5} for the Einasto and NFW profiles, respectively. An alternative parametrization of the Einasto profile [15] leads to $J_{E_2} = 1.51 \times 10^{21}$ GeV^2 cm^{-5}. The J factor values for the regions of interest (ROI) considered here are reported in Table I in the Supplemental Material [16].

We reexamine the GC region to search for a DM annihilation signal in the inner Galactic halo [10] using the full statistics from 10 years of GC observations with the initial four telescopes of the H.E.S.S. instrument [17]. We perform a new search with an improved data analysis procedure [18] and a two-dimensional (2D) likelihood-based method using both the spectral and spatial characteristics of the DM annihilation signal with respect to background.

Data analysis.—The present data analysis makes use of 254 h (live time) of GC observations during the years 2004–2014 by H.E.S.S. Pointing positions are chosen with radial offsets from 0.7° to 1.1° from the GC. Standard quality selection criteria are applied to the data to select γ-ray events [17], additionally requiring observational zenith angles lower than 50° to minimize systematic uncertainties in the event reconstruction. The mean zenith angle of the selected observations is 19°.

The DM signal is analyzed in ROIs defined as annuli of 0.1° width each and centered at the GC, with inner radii

from 0.3° to 0.9° in radial distance from the GC, hereafter referred to as the ON regions. In order to minimize contamination from the above-mentioned astrophysical emission, a band of ±0.3° in Galactic latitude is excluded along the Galactic plane. (Interestingly, this enables us to derive constraints that do not strongly depend on the central DM density distribution, which is poorly known in the innermost few tens of parsecs of the GC.) The background events are selected in OFF regions defined for each observation as annuli symmetric to the ON regions with respect to the pointing position (see Fig. 1 in the Supplemental Material [16]). The OFF regions are expected to contain signal events as well, which decreases any potential excess in the ON regions. The OFF regions are always taken sufficiently far from the ON regions to obtain a significant contrast in the DM annihilation signal between the ON and OFF regions. [This analysis method is unable to probe cored profiles (such as isothermal or Burkert profiles). A dedicated observation strategy is required as shown in Ref. [12]]. We considered here the above-mentioned DM profiles for which the OFF regions contain always fewer DM events than the ON regions. A Galactic diffuse emission has been detected by the *Fermi* satellite [19,20] and H.E.S.S. [21]. Any potential γ-ray contribution from the Galactic diffuse emission is considered as part of the signal, which makes the analysis conservative as long as no signal is detected.

We perform a 2D binned Poisson maximum likelihood analysis, which takes full advantage of the spatial and spectral characteristics of the DM signal with respect to the background. We use 70 logarithmically spaced energy bins from 160 GeV to 70 TeV, and seven spatial bins corresponding to ROIs defined as the above-mentioned annuli of 0.1° width. For a given DM mass $m_{\rm DM}$ and annihilation channel, the joint likelihood is obtained by the product of the individual Poisson likelihoods over the spatial bins i and the energy bins j. It reads

$$\mathcal{L}(m_{\rm DM}, \langle\sigma v\rangle) = \prod_{i,j} \mathcal{L}_{ij},$$
$$\text{with} \quad \mathcal{L}_{ij}(\mathbf{N}_S, \mathbf{N}_B | \mathbf{N}_{\rm ON}, \mathbf{N}_{\rm OFF}, \boldsymbol{\alpha}) = \frac{(N_{S,ij} + N_{B,ij})^{N_{{\rm ON},ij}}}{N_{{\rm ON},ij}!} e^{-(N_{S,ij}+N_{B,ij})}. \quad (3)$$

$N_{S,ij} + N_{B,ij}$ is the expected total number of events in the spatial bin i and spectral bin j of the ON regions. The expected number of signal events $N_{S,ij}$ is obtained by folding the theoretical number of DM events by the instrument response function of H.E.S.S. for this data set. $N_{B,ij}$ is the number of background events expected in the spatial bin i and spectral bin j. $N_{{\rm ON},ij}$ and $N_{{\rm OFF},ij}$ are the number of observed events in the ON and OFF regions, respectively. $N_{B,ij}$ is extracted from the OFF regions and given by $N_{B,ij} = \alpha_i N_{{\rm OFF},ij}$. The parameter $\alpha_i = \Delta\Omega_i / \Delta\Omega_{\rm OFF}$ refers to the ratio between the angular size of the ON region i and the OFF region. In our case, this ratio

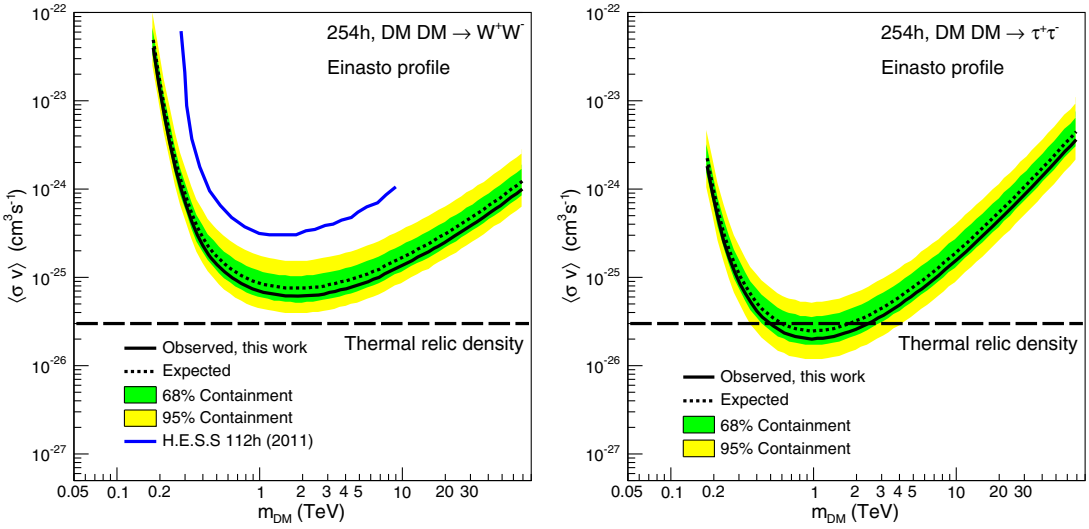

FIG. 1. Constraints on the velocity-weighted annihilation cross section $\langle\sigma v\rangle$ for the W^+W^- (left panel) and $\tau^+\tau^-$ (right panel) channels derived from observations taken over 10 years of the inner 300 pc of the GC region with H.E.S.S. The constraints for the $b\bar{b}$, $t\bar{t}$, and $\mu^+\mu^-$ channels are given in Fig. 4 in Supplemental Material [16]. The constraints are expressed as 95% C.L. upper limits as a function of the DM mass $m_{\rm DM}$. The observed limit is shown as a black solid line. The expectations are obtained from 1000 Poisson realizations of the background measured in blank-field observations at high Galactic latitudes. The mean expected limit (black dotted line) together with the 68% (green band) and 95% (yellow band) C.L. containment bands are shown. The blue solid line corresponds to the limits derived in a previous analysis of 4 years (112 h of live time) of GC observations by H.E.S.S. [10]. The horizontal black long-dashed line corresponds to the thermal relic velocity-weighted annihilation cross section (natural scale).

is equal to 1 since each OFF region is taken symmetrically to the ON region from the pointing position (including corrections for the camera acceptance). Consequently, they have the same angular size and exposure. $\mathbf{N}_S$, $\mathbf{N}_B$, $\mathbf{N}_{\mathrm{ON}}$, $\mathbf{N}_{\mathrm{OFF}}$, and α are the vectors corresponding to the quantities previously defined. Constraints on $\langle\sigma v\rangle$ are obtained from the likelihood ratio test statistic given by $\mathrm{TS} = -2\ln[\mathcal{L}(m_{\mathrm{DM}}, \langle\sigma v\rangle)/\mathcal{L}_{\mathrm{max}}(m_{\mathrm{DM}}, \langle\sigma v\rangle)]$, which, in the high statistics limit, follows a χ^2 distribution with 1 degree of freedom [22]. Values of $\langle\sigma v\rangle$ for which TS is higher than 2.71 are excluded at the 95% confidence level (C.L.).

Results.—We find no significant γ-ray excess in any of the ON regions (ROIs) with respect to the OFF regions [16]. We derive upper limits on $\langle\sigma v\rangle$ at a 95% C.L. for WIMPs with masses from 160 GeV to 70 TeV, annihilating into quark ($b\bar{b}$, $t\bar{t}$), gauge boson (W^+W^-), and lepton ($\mu^+\mu^-$, $\tau^+\tau^-$) channels. The γ-ray spectrum from DM annihilation in the channel f is computed by using the tools available from Ref. [15]. The left panel of Fig. 1 shows the observed 95% C.L. upper limits for the W^+W^- channel and the Einasto profile. The expected limits are obtained from 1000 Poisson realizations of the background obtained through observations of blank fields at high latitudes where no signal is expected (see the Supplemental Material [16]). The mean expected upper limit together with the 68% and 95% containment bands are plotted. The limits reach 6×10^{-26} cm^3 s^{-1} for a DM particle of mass 1.5 TeV. We obtain a factor of 5 improvement compared with the results of Ref. [10]. The larger data set and the improved data analysis method contribute to the increase of the sensitivity of the analysis presented here. In the right panel of Fig. 1, the observed 95% C.L. upper limit is shown for the $\tau^+\tau^-$ channel together with the expected limits. The limits reach $\langle\sigma v\rangle$ values expected for dark matter annihilating at the thermal-relic cross section. The observed upper limits together with the expectations are given for the $b\bar{b}$, $t\bar{t}$, and $\mu^+\mu^-$ channels, respectively, in Fig. 4 in the Supplemental Material [16]. The limits obtained in the leptonic channels ($\mu^+\mu^-$, $\tau^+\tau^-$) are comparatively strong with respect to those in the quark channels ($b\bar{b}$, $t\bar{t}$). This mainly comes from the relatively soft measured γ-ray spectra compared to the hard ones stemming from the leptonic annihilation channels. In the left panel of Fig. 2, the impact of the DM distribution hypothesis on the observed upper limit is shown for the NFW profile and an alternative parametrization of the Einasto profile extracted from Ref. [15].

The right panel of Fig. 2 shows a comparison with the current constraints obtained from the observations of the Major Atmospheric Gamma Imaging Cherenkov (MAGIC) ground-based Cherenkov telescope instrument towards the Segue 1 dwarf galaxy [24] (the J factor of Segue 1 used in Ref. [24] could be overestimated by a factor of 100 as shown in Ref. [26]), the combined analysis of four dwarf galaxies observed by H.E.S.S. [25], and the observations of 15 dwarf galaxy satellites of the Milky Way by the *Fermi* satellite [23].

Summary.—We present a new analysis of the inner halo of the Milky Way using 10 years of observation of the GC (254 h of live time) by phase 1 of H.E.S.S. and a novel

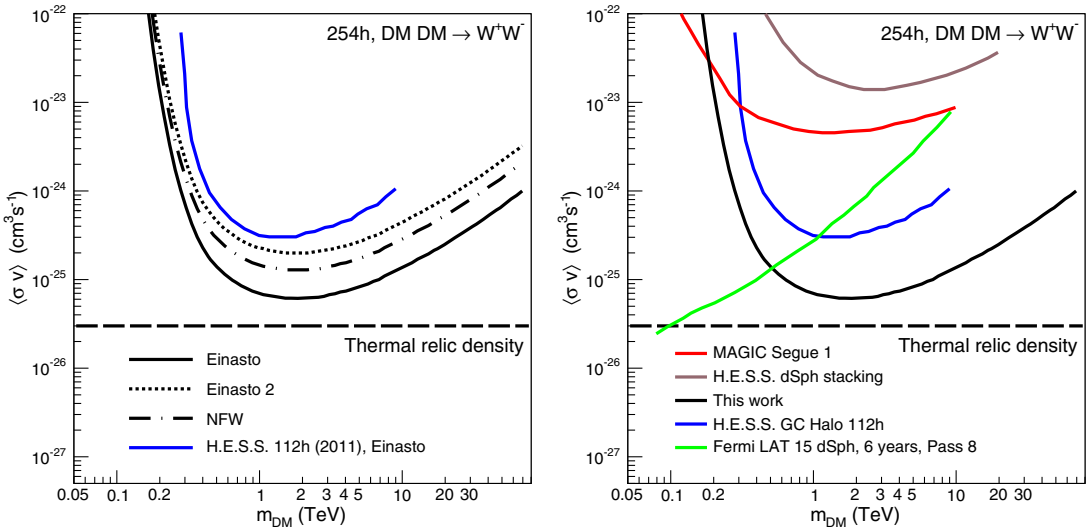

FIG. 2. Left: impact of the DM density distribution on the constraints on the velocity-weighted annihilation cross section $\langle\sigma v\rangle$. The constraints expressed in terms of 95% C.L. upper limits are shown as a function of the DM mass m_{DM} in the W^+W^- channels for the Einasto profile (solid black line), another parametrization of the Einasto profile (dotted black line), and the NFW profile (long dashed-dotted black line), respectively. Right: comparison of the constraints on the W^+W^- channels with the previous published H.E.S.S. limits from 112 h of observations of the GC [10] (blue line), the limits from the observations of 15 dwarf galaxy satellites of the Milky Way by the *Fermi* satellite [23] (green line), the limits from 157 h of observations of the dwarf galaxy Segue 1 [24] (red line), and the combined analysis of observations of 4 dwarf galaxies by H.E.S.S. [25] (brown line).

statistical analysis technique using a 2D maximum likelihood method. We find no evidence of a gamma-ray excess and thus exclude a velocity-weighted annihilation cross section of 6×10^{-26} cm^3 s^{-1} for DM particles with a mass of 1.5 TeV annihilating in the W^+W^- channel for an Einasto profile. These are the most constraining limits obtained so far in the TeV mass range. Our constraints surpass the *Fermi* limits for particle masses above 400 GeV in the W^+W^- channel. The strongest limits are obtained in the $\tau^+\tau^-$ channel at 2×10^{-26} cm^3 s^{-1} for a DM particle mass of 1 TeV. For the first time, observations with a ground-based array of imaging atmospheric Cherenkov telescopes are able to probe the thermal relic annihilation cross section in the TeV DM mass range.

The upcoming searches with H.E.S.S. towards the inner Galactic halo will benefit from additional observations of phase 2 of H.E.S.S., which aims for an energy threshold lowered down to several tens of GeV and improved sensitivity in the TeV energy range. Higher Galactic latitude observations will allow increasing the source region size and in turn reduce the impact of the uncertainty of the DM distribution in the inner kiloparsec of the GC. Within the next few years, searches with H.E.S.S. observations are expected to explore in-depth the WIMP paradigm for TeV DM particles.

The support of the Namibian authorities and of the University of Namibia in facilitating the construction and operation of H.E.S.S. is gratefully acknowledged, as is the support by the German Ministry for Education and Research (BMBF), the Max Planck Society, the French Ministry for Research, the CNRS-IN2P3 and the Astroparticle Interdisciplinary Programme of the CNRS, the U.K. Science and Technology Facilities Council (STFC), the IPNP of Charles University, the Polish Ministry of Science and Higher Education, the South African Department of Science and Technology and National Research Foundation, and the University of Namibia. We appreciate the excellent work of the technical support staff in Berlin, Durham, Hamburg, Heidelberg, Palaiseau, Paris, Saclay, and Namibia in the construction and operation of the equipment.

[*] Deceased.
[†] To whom all correspondence should be addressed.
contact.hess@hess-experiment.eu
[‡] valentin.lefranc@cea.fr
[§] emmanuel.moulin@cea.fr

[1] R. Adam *et al.* (Planck Collaboration), arXiv:1502.01582.
[2] G. Jungman, M. Kamionkowski, and K. Griest, Phys. Rep. **267**, 195 (1996).
[3] L. Bergstrom, Rep. Prog. Phys. **63**, 793 (2000).
[4] G. Bertone, D. Hooper, and J. Silk, Phys. Rep. **405**, 279 (2005).
[5] F. Aharonian *et al.* (H.E.S.S. Collaboration), Astron. Astrophys. **425**, L13 (2004).
[6] F. Aharonian *et al.* (H.E.S.S. Collaboration), Astron. Astrophys. **503**, 817 (2009).
[7] F. Aharonian *et al.* (H.E.S.S. Collaboration), Astron. Astrophys. **432**, L25 (2005).
[8] F. Aharonian (H.E.S.S. Collaboration), Astron. Astrophys. **483**, 509 (2008).
[9] F. Aharonian *et al.* (H.E.S.S. Collaboration), Nature (London) **439**, 695 (2006).
[10] A. Abramowski *et al.* (H.E.S.S. Collaboration), Phys. Rev. Lett. **106**, 161301 (2011).
[11] V. Lefranc, E. Moulin, P. Panci, and J. Silk, Phys. Rev. D **91**, 122003 (2015).
[12] A. Abramowski *et al.* (H.E.S.S. Collaboration), Phys. Rev. Lett. **114**, 081301 (2015).
[13] V. Springel, S. D. M. White, C. S. Frenk, J. F. Navarro, A. Jenkins, M. Vogelsberger, J. Wang, A. Ludlow, and A. Helmi, Nature (London) **456**, 73 (2008).
[14] J. F. Navarro, C. S. Frenk, and S. D. M. White, Astrophys. J. **490**, 493 (1997).
[15] M. Cirelli, G. Corcella, A. Hektor, G. Hütsi, M. Kadastik, P. Panci, M. Raidal, F. Sala, and A. Strumia, J. Cosmol. Astropart. Phys. 03 (2011) 051; 10 (2012) E01.
[16] See Supplemental Material at http://link.aps.org/supplemental/10.1103/PhysRevLett.117.111301 for more details.
[17] F. Aharonian *et al.* (H.E.S.S. Collaboration), Astron. Astrophys. **457**, 899 (2006).
[18] M. de Naurois and L. Rolland, Astropart. Phys. **32**, 231 (2009).
[19] M. Ackermann *et al.* (Fermi-LAT Collaboration), Astrophys. J. **750**, 3 (2012).
[20] M. Ackermann *et al.* (Fermi-LAT Collaboration), Astrophys. J. **799**, 86 (2015).
[21] A. Abramowski *et al.* (H.E.S.S. Collaboration), Phys. Rev. D **90**, 122007 (2014).
[22] W. A. Rolke, A. M. Lopez, and J. Conrad, Nucl. Instrum. Methods Phys. Res., Sect. A **551**, 493 (2005).
[23] M. Ackermann *et al.* (Fermi-LAT Collaboration), Phys. Rev. Lett. **115**, 231301 (2015).
[24] J. Aleksic *et al.* (MAGIC Collaboration), J. Cosmol. Astropart. Phys. 02 (2014) 008.
[25] A. Abramowski *et al.* (H.E.S.S. Collaboration), Phys. Rev. D **90**, 112012 (2014).
[26] V. Bonnivard *et al.*, Mon. Not. R. Astron. Soc. **453**, 849 (2015).